SAND99-1514J

~~PRL DRAFT 6/10/99 15:00~~

# Z-Pinch Generated X-Rays Demonstrate Indirect-Drive ICF Potential*

T. W. L. Sanford, R. E. Olson, G. A. Chandler, M. S. Derzon, D. E. Hebron, R. C. Mock, R. J. Leeper, M. K. Matzen, T. J. Nash, L. E. Ruggles, W. W. Simpson, K. W. Struve, and R. A. Vesey
*Sandia National Laboratories*

R. L. Bowers, and D. L. Peterson
*Los Alamos National Laboratory*



## Abstract

Hohlraums (measuring 6-mm in diameter by 7-mm in height) have been heated by x-rays from a z-pinch. Over measured x-ray input powers P of 0.7 to 13 TW, the hohlraum radiation temperature T increases from ~ 55 to ~130 eV, and is in agreement with the Planckian relation $P \sim T^4$. The results suggest that indirect-drive ICF studies involving NIF relevant pulse shapes and <2-mm diameter capsules can be studied using this arrangement.

Implosion and ignition of an indirectly-driven ICF capsule operating near a Fermi-degenerate isentrope requires initial Planckian-radiation-drive temperatures of 70-90 eV to be present for a duration of ~10 ns prior to a multi-step drive that reaches a peak temperature of 250-300 eV [1, 23, 24]. Such capsules are being designed [2] for high-power z-pinch generators [3, 4]. In this letter, we show that the initial *foot-pulse* x-ray drive has been demonstrated for the first time in a *static-wall hohlraum* geometry [2-4] suitable for imploding < 2-mm-diameter capsules on the 20-MA Z generator [5]. The experimental arrangement uses a single-feed, one-sided, x-ray drive on Z, as is illustrated in the schematic of Fig. 1. In the schematic, a hohlraum cylinder with gold walls measuring 6-mm in diameter by 7-mm height is placed on-axis above a x-ray producing magnetic z-pinch [6]. X-rays enter the hohlraum through a REH (radiation entrance hole) and heat the gold walls of the hohlraum. The x-rays are generated by the thermalization of the kinetic energy acquired when a surrounding array of wires collides with a target (Fig. 1B) in the z-pinch. In this arrangement, the wires (which are made of tungsten) form an annular plasma radiation case [7] at the time they strike the target (first strike). The high-atomic-number radiation case traps a fraction of the x-rays produced (as in a *dynamic-hohlraum* configuration [3,4,8]) and

*Work supported by U.S. DOE Contract No. DE-AC04-94AL85000

## DISCLAIMER

enables the trapped radiation to be channeled into the hohlraum, producing the *foot-pulse* drive. A secondary pulse leading to a *peak pulse* is generated when the imploding array plus target stagnates on axis, as illustrated in Fig. 1C. Radiation from both the interior (c in Fig. 1C) and exterior (a and b in Fig. 1C) of the radiation case then flows into the hohlraum.

The experiments discussed here show that as final, on-axis stagnation is approached, the REH closes, likely due to tungsten and/or gold plasma filling the REH and subsequently limiting the x-rays reaching the hohlraum. Calculations [9] suggest filling the hohlraum with a low-density foam might generate a back pressure, which would limit the closure. Experiments with foam-filled hohlraums are planned for the future. In the vacuum hohlraums discussed here, however, the potential for a scalable *peak-pulse* capability was studied by removing the target and allowing the radiation from the pinch to directly irradiate the interior of the hohlraum, thereby reducing the time available for REH closure. The radiation generated with this modified *static-wall-hohlraum* geometry provides a lower bound than that which can be delivered to the hohlraum, because it does not take advantage of the x-rays trapped within an imploding target structure (c in Fig. 1C). In this modified configuration, the hohlraum is sensitive only to the x-rays generated from the exterior of the opaque tungsten pinch, namely from its top and a limited portion of its side (a and b in Fig. 1C), but not from its hot interior (c in Fig. 1C) as in the full configuration with the target. Nevertheless, the experiment reported on here demonstrates, for the first time, the generation of a temperature significantly in excess of 100 eV for an x-ray driven hohlraum with static walls, and, importantly, the potential for producing a *peak-pulse* from a z-pinch generator that would be needed for studying ignition physics in the next generation (~50 MA) z-pinch driver [10].

The hohlraum used in the experiments is a thin-walled (25.4-μm thickness), gold cylinder that is axially centered above the z-pinch target (Fig. 1A). The temperature of its inside wall, midway between its bottom and top, is measured with two independent diagnostics, each of which view the interior of the hohlraum through the same ~3-mm diameter aperture on its lateral side, but at $\pm 20^{\circ}$ about the normal to the hole in the horizontal plane. In one diagnostic, the temperature is measured using a set of twelve PIN-diodes that are mounted downstream from a transmission-grating-spectrometer, which are positioned to be sensitive to x-rays in discrete energy channels that span 100 to 600 eV [11]. In the other diagnostic, the temperature is measured using a total-energy bolometer [12] and a set of K- and L-edge filtered photocathode detectors (XRDs) that are sensitive to x-rays in four discrete channels that also cover a similar energy range [13]. Plasma closure of the diagnostic hole with time is measured with a multi-filtered, fast-framing, PIN-hole camera, which is sensitive to x-rays in four discrete channels covering 100 to 600 eV [14]. Over the range of

hohlraum temperatures measured in this experimental series ( ~55 to ~130 eV), the radius of the hole is measured to close by 0.25±0.05 mm at the time of peak temperature, and is accounted for in the evaluation of the temperature. Relative comparisons between the radiation detectors within each diagnostic set indicate no measurable deviation in internal azimuthal symmetry of the hohlraum with time [15]. The peak temperature extracted from either diagnostic set agrees to within (2±3)% when averaged over the 14 shots. Here the uncertainty refers to the RMS shot-to-shot variation. The radiation entering the hohlraum is estimated by an additional suite of on-axis diagnostics [3, 8] that view the source through the REH when the hohlraum is not present. These diagnostics include a total-energy bolometer , a filtered XRD set, and filtered fast-framing pin-hole cameras similar to those detectors of the horizontal diagnostic sets.

The target used (Fig. 1A) is a copper-walled cylinder 2-μm thick, with a diameter of 8 mm, and a gold bottom. The diameter is matched to its implosion velocity after first strike in such a way that *foot-pulse* radiation should be generated for ~10 ns before final stagnation occurs. Copper is selected because its high density thermalizes the incident wire-plasma kinetic energy in a short radial distance and for its sub-keV opacity characteristics, which allow the target interior to fill with radiation before final stagnation occurs. The gold bottom provides a high albedo for increased radiation containment. The interior of the cylinder is filled either with a 10-mg/cc CH foam or vacuum. Once the radiation exits the interior wall of the copper shell, in the case of a vacuum interior, or once the foam fill has become sufficiently ionized, the radiation exits the imploding target through the top, 5.8-mm-diameter REH that connects the target with the hohlraum. The radiation generated from the target exterior is monitored by bolometers, filtered XRDs, and a fast-framing pin-hole camera that view the target through a diagnostic aperture in the anode structure of the current-return structure (Fig. 1A). The target bottom is electrically isolated from the cathode current-return path by a 1-mm gap in order to minimize preheating the copper shell prior to wire plasma impacting the shell.

Because the x-ray power from a z-pinch increases with wire number and associated reduction in interwire spacing [7, 16-18], the initial set of experiments with this hohlraum and target geometry used a single array of ~480 tungsten wires. The wires measured 20-mm in length and were mounted at a diameter of 40 mm. The associated interwire spacing was ~0.26 mm, which corresponds to the limit of current wire-load construction capability. For these small spacings, the wires are expected to form a quasi-plasma-shell prior to first strike [7]. The mass of the wire array was varied from 1.5 mg/cm to 4 mg/cm, over a range calculated to maximize the on-axis radiation. In all cases the power delivered to the target was insufficient to cause the foam to burn through significantly (ie, to become sufficiently ionized

and, hence, transparent to the x-rays) prior to stagnation. Near stagnation, however, the foam did burn through, delivering ~1 TW into the REH. The peak hohlraum temperature increased from ~55 to ~70 eV as the array-mass increased. Figure 2 illustrates these features at the highest array-mass explored. In the figure, the thick curve corresponds to the power measured off-axis and external to the target, with its early time peak and later peak corresponding to first strike and final stagnation, respectively. In contrast, the thin curve in Fig. 2 shows that the hohlraum becomes heated only as stagnation is approached. In these experiments, the current-return structure had a number of apertures that degraded the azimuthal symmetry of the implosion and resulting first-strike power. Moreover, these initial experiments showed that the radiation generated in the lower portion of the target was being absorbed before exiting the REH. Additionally, nesting wire arrays (ie, placing an additional array of wires interior to an outer array) was found to increase the power generated in targetless implosions [19].

Thus, in a second set of experiments, (1) the apertures in the current return can were eliminated (except for a small 3-mm-diameter aperture designed to monitor the timing of the off-axis target radiation), (2) the length of the wires was reduced from 20 mm to ~9 mm thereby increasing the power per unit length delivered to the target [5], and (3) nested wire arrays were used. Through these changes, the power delivered to the target was increased so that for an effective array mass of 3 mg/cm, where 2 mg in 240 wires was allocated to a diameter of 40 mm and 1 mg in 120 wires was allocated to a diameter of 20 mm, the foam burned through soon after the first strike, generating about four times the on-axis power incident into the hohlraum, and raising the hohlraum temperature to a peak of 85 eV, ~10 ns prior to final stagnation (solid curve in Fig. 3). The energy distribution between first strike and stagnation is measured to be Planckian, as illustrated in Fig. 4. Eliminating the foam fill reduces the delay of the radiation delivered to the hohlraum after first strike (dashed curve in Fig. 3), and illustrates the flexibility in producing differing temperature profiles by varying the density of the fill. Relative to the temperature pulse generated with only vacuum, the power being produced in compressing the foam helps to maintain the duration and temperature level of the *foot pulse* prior to stagnation. Importantly, the initial temperature profile generated with the foam fill corresponds approximately to the conditions required for a *foot-pulse* drive for ICF ignition prior to a *first-step-pulse* drive. This correspondence is demonstrated by the comparison with two repesentative *foot pulse* drives calculated for NIF and labeled in Fig. 3 as W [23] and D [24]. With such a *foot-pulse* source, ablator physics [1], helium-filled wall tamping [2], hole-closure, and other issues associated with ICF implosions on NIF can be studied under realistic pulse-temperature, pulse-length, and hohlraum-size conditions.

Subsequent experiments with a single array showed little benefit from the nesting. Thus, the main improvement was due to the reduced length and increased symmetry. Shown also in Fig. 3 is a lack of a significant temperature increase as stagnation is approached. An increase in x-ray power is required to demonstrate the configuration's utility in producing a *first-step* and subsequent steps leading to a *peak pulse* that would be suitable for scaling to ignition conditions in a larger z-pinch generator. Two-dimensional Eulerian-Radiation-Magnetohydrodynamic -Code (E-RMHC) simulations in the r-z plane [20], which take into account the Rayleigh-Taylor (RT) instabilities, indicate that as final stagnation is approached, the on-axis power being delivered to the hohlraum should have increased by a factor of ~2.5 relative to the power generated at first strike. This increase would correspond to a 25% rise in hohlraum temperature relative to that measured at first strike, and would be suitable for simulating a *first-step-pulse* drive (Fig. 3). This expected rise, however, is not observed here. As mentioned earlier, blockage of the REH by tungsten wire plasma sliding across the aperture is now thought to be responsible for this lack of temperature enhancement at stagnation [9], rather than loss of radiation due to a leaky radiation case or mixing of the tungsten in the foam that would increase the opacity of the target interior. E-RMHC calculations that now include the hohlraum in the simulation, suggest that utilizing low-density, low-opacity, foam fill within the hohlraum should eliminate the blockage.

In order to demonstrate the potential of using a *static-walled-hohlraum* to simulate also a *first-step pulse* in this experimenal series, the target was removed and a bare pinch studied. In this manor, a *first-step pulse* could be simulated prior to REH closure. (In future experiments, the *first-step pulse* in combination with a *foot pulse* will be examined by adding the target back in, with the gradual addition of material to the target and hohlraum structure. In the process, tamping the REH for increased pulse duration will be explored.) For this bare-pinch configuration, the length of the wires was further reduced to ~7mm and the diameters of the outer- and inner-wire-array nest decreased to 35 mm and 17.5 mm, respectively, in order to reduce the growth of the RT instability [21]. With these changes, the peak power measured exiting the REH increased by a factor of ~4 to 13±2 TW. The associated hohlraum temperature measured at stagnation increased to 123±5 eV, roughly the conditions required of a *first-step-pulse* (Fig. 3). The uncertainty in the power corresponds to the RMS variation measured among three independent bolometers, and that of the temperature corresponds to the systematic uncertainty due to the hole-closure correction and to diagnostic response. The temperature agrees with the value of 118 eV calculated with the static, 3D-radiosity code Lightscape [22] (Fig. 5), assuming a wall albedo of 0.8 (estimated for these conditions) and a uniform intensity across the REH. Taking into account the minor variations in the hohlraum diagnostic apertures, the temperature and associated on-axis

power measured over the experimental series (Fig. 6) are in excellent agreement with that expected from the Planckian relation $P \sim T^4$ (where P is the input power and T is the hohlraum temperature).

For the bare pinch geometry the hohlraum had in addition to the lateral diagnostic hole, a diagnostic hole in its top that permitted the pinch to be simultaneously imaged in combination with a half-moon radiation shield of 2-mm diameter positioned 1.5 mm above the REH on axis. Calculations with the radiosity code indicate that owing to (1) the radiation loss from the holes, (2) the asymmetry generated from the one-sided drive, and (3) the radiation blockage by the shield, the axial temperature gradient across the ~3-mm axial length being monitored on the inside of the hohlraum wall decreases at the rate of 4.3% per mm (solid curve in Fig. 5). The measured gradient of (4.6±0.6)% per mm is consistent with this calculation. If both diagnostic holes had been closed, the temperature of the hohlraum would have been increased by 10 eV to 133 eV at stagnation (dashed curve in Fig. 5). On the other hand, distributing the wire mass in two independent pinches of approximately half the length of the single one (in order to maintain a similar over all load inductance), with the hohlraum sandwiched between the two pinches, should generate approximately the same on-axis power from each pinch, because the on-axis power is primarily produced from the ends of the pinch (Fig. 1C). In this case, the x-ray power incident on the hohlraum would be doubled. The calculated temperature profile associated with this single-feed, two-sided, x-ray drive (as in the geometry shown in Fig. 3 of Ref. 2) is illustrated by the dot-dashed curve in Fig. 5. For this geometry, the temperature of the hohlraum could be increased to ~150 eV at its center, with the temperature gradient significantly reduced. Such a configuration would be suitable for studying implosion dynamics of z-pinch driven capsules of diameters <2 mm, where thermonuclear neutrons in excess of $10^8$ may be produced and measured, as well as x-rays from tracer elements that could monitor the dynamics and symmetry of the implosion and hot deuteron core. Moreover, scaling this concept to a similar, single-feed, double-sided, 50-MA driver, which is characteristic of the next generation z-pinch driver being considered [10], could provide conditions suitable for studying ignition physics.

In conclusion, this *static-wall-hohlraum* experimental series has demonstrated (1) the generation of a *foot-pulse* necessary for ICF ignition and propagation burn, (2) a present limitation in combining a *foot pulse* with a *first-step pulse* , which may be avoided by the use of low-opacity foam-filling within the hohlraum, and (3) the potential for x-ray driven capsule implosion studies on the existing Z generator as well as on a next generation z-pinch driver.

## References:


[1] R. E. Olson, J. L. Porter, G. A. Chandler, *et al.*, *Phys. Plasmas* 4, 1818 (1997).

[2] R. E. Olson, G. A. Chandler, M. S. Derzon, et al., *Fusion Technology*, 35, 260 (1999).

[3] R.J. Leeper, T.E. Alberts, J.R. Asay, *et al.*, "Z-pinch Driven Inertial Confinement Fusion Target Physics Research at Sandia National Laboratoies", proceedings 17th IAEA Fusion Energy Conference, Yokohama, Japan, Oct. 19-24, 1998, International Atomic Energy Agency, Vienna.

[4] M. K. Matzen, C. Deeney, R. J. Leeper, et al, *Plasma Phys. Control. Fusion* 41, 175 (1999).

[5] R. B. Spielman, C. Deeney, G. A. Chandler, et al., *Phys. Plasmas*, 5, 2105 (1998).

[6] N. R. Pereira and J. Davis, *J. Appl. Phys.* 64, R1 (1988).

[7] T. W. L. Sanford, R. B. Spielman, G. O. Allshouse, *et al.*, *IEEE Trans. Plasma Sci.*, 26, 1086 (1998).

[8] T. J. Nash , M. S. Derzon, G. A. Chandler, et al, *Phys. Plasmas* 6, 2023 (1999).

[9] R. L. Bowers et al, to be published and M. S. Derzon Sand report.

[10] K. W. Struve, J. P. Corley, D. L. Johnson, et al.,"ZX Pulsed-Power Design," to be published in the *Proceedings of the International Pulsed Power Conference, 1999, Monterey, CA* (June 1999).

[11] J. L. Porter, *Am. Phys. Soc.* 44, 1948 (1997).

[12] R. B. Spielman, J. S. De Groot, T. J. Nash, et al, *Dense z-Pinches* (3rd International Conference, London, UK, 1993), AIP Conference Proceedings 299, editors H. Haines and A. Knight, American Institute of Physics, New York 1994, L.C. Catalog Card No. 93-74569, pages 404-420.

[13] G. A. Chandler, J. Hubert, J. Bailey, *et al.*, *Rev. Sci. Instrum.* 63, 4828 (1992).

[14] L. E. Ruggles, R. B. Spielman, J. L. Porter, and S. P. Breeze, *Rev. Sci. Instrum.*, 66, 712,(1995).

[15] R. E. Olson, G. A. Chandler, T. W. L. Sanford, et al, *Am. Phys. Soc.* 43, 1882 (1998).

[16] T. W. L. Sanford, G. O. Allshouse, B. M. Marder, *et al.*, *Phys. Rev. Lett.* 77, 5063 (1996).

[17] C. Deeney, T. J. Nash, R. B. Spielman, et al, *Phys. Rev. E* 56,5945 (1997).

[18] T. W. L. Sanford, R. C. Mock, T. J. Nash, et al, *Phys. Plasmas* 6, 1270 (1999).

[19] C. Deeney, M. R. Douglas, R. B. Spielman, et al, *Phys. Rev. Lett.* 81, 4883 (1998).

[20] D. L. Peterson, R. L. Bowers, W. Matuska, et al, *Phys. Plasmas* 6, 2178 (1999).

[21] T. W. L. Sanford, R. C. Mock, R. B. Spielman, *et al.*, *Phys. Plasmas* 5, 1355 (1998).

[22] Michael F. Cohen and John R. Wallace, "Radiosity and Realistic Image Synthesis", Academic Press, Boston, MA, (1993).

[23] D. C. Wilson, P. A. Bradley, N. M. Hoffman, et al, *Phys. Plasmas* 5, 1953 (1998).

[24] T. R. Dittrich, S. W. Haan, M. M. Marinak, et al, *Phys. Plasmas* 5, 3708 (1998).

*Sandia is a multiprogram laboratory operated by the Sandia Corporation, a Lockheed Martin Company, for the U.S. Department of Energy under Contract No. DE-AC04-94AL85000.

## Figure Captions:

1. Schematic of *static-wall-hohlraum* concept illustrating (A) initial conditions, (B) radiation flow at first strike, and (C) radiation flow near final stagnation. (A) shows also the locations of the target, hohlraum, and on-axis diagnostics, and the position of the REH. In (A), K and A refer to the cathode and anode surfaces, respectively.

2. Relative x-ray power measured external to the target and the associated hohlraum temperature measured for Shot Z201, which had a wire mass of 4 mg/cm.

3. Hohlraum temperature measured for a 10 mg/cc foam-filled target (thick solid curve) and that measured with no foam (thin dashed curve), corresponding to Shots Z251 and Z250, respectively. The temperature profile of Shot Z251 relative to Shot Z250 has been left shifted by 3.5 ns. Hashed region illustrates a limited range of NIF drive requirements for 2-mm sized capsules having Be ablators. (W) corresponds to the Be-300 capsule design of Ref. 23 and (D) the reduced-scale capsule design of Ref. 24.

4. X-ray energy-distribution measured with the transmission-grading spectrometer at peak temperature, for the foam-filled shot Z251 (see Fig. 3). The solid curve corresponds to a 85 eV Planckian distribution.

5. Calculated Lightscape temperature profiles for the interior hohlraum wall opposite the lateral diagnostic hole for (A) a one-sided drive with a lateral and top diagnostic hole corresponding to the conditions of shot Z387, (B) a one-sided drive with no diagnostic holes, and (C) a two-sided drive with one lateral diagnostic hole. 13 TW was assumed for each input drive. Shown also is the measured temperature from Shot Z387 corresponding to the conditions of (A).

6. Measured hohlraum temperature as a function of the measured, on-axis, x-ray power for the indicated shot pairs, with and without the hohlraum present. Shown also is that expected from the Planckian scaling relation , using the Lightscape calculation with a 13-TW normalization point.

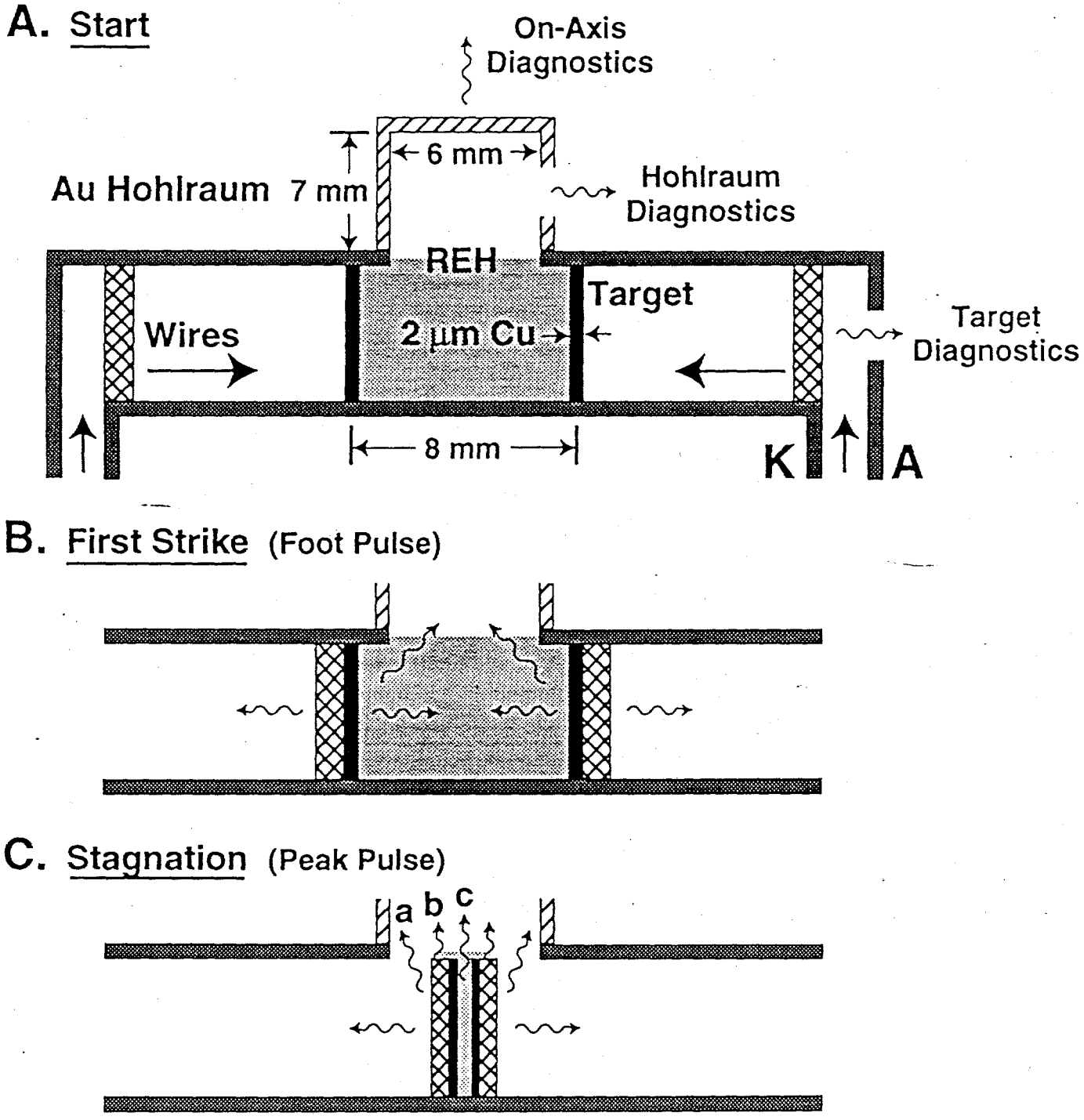
A. Start
On-Axis
Diagnostics
6 mm
Au Hohlraum 7 mm
Hohlraum
Diagnostics
REH
Target
Wires
2 μm Cu
Target
Diagnostics
8 mm
K
A
B. First Strike (Foot Pulse)
C. Stagnation (Peak Pulse)
a b c

Fig 1

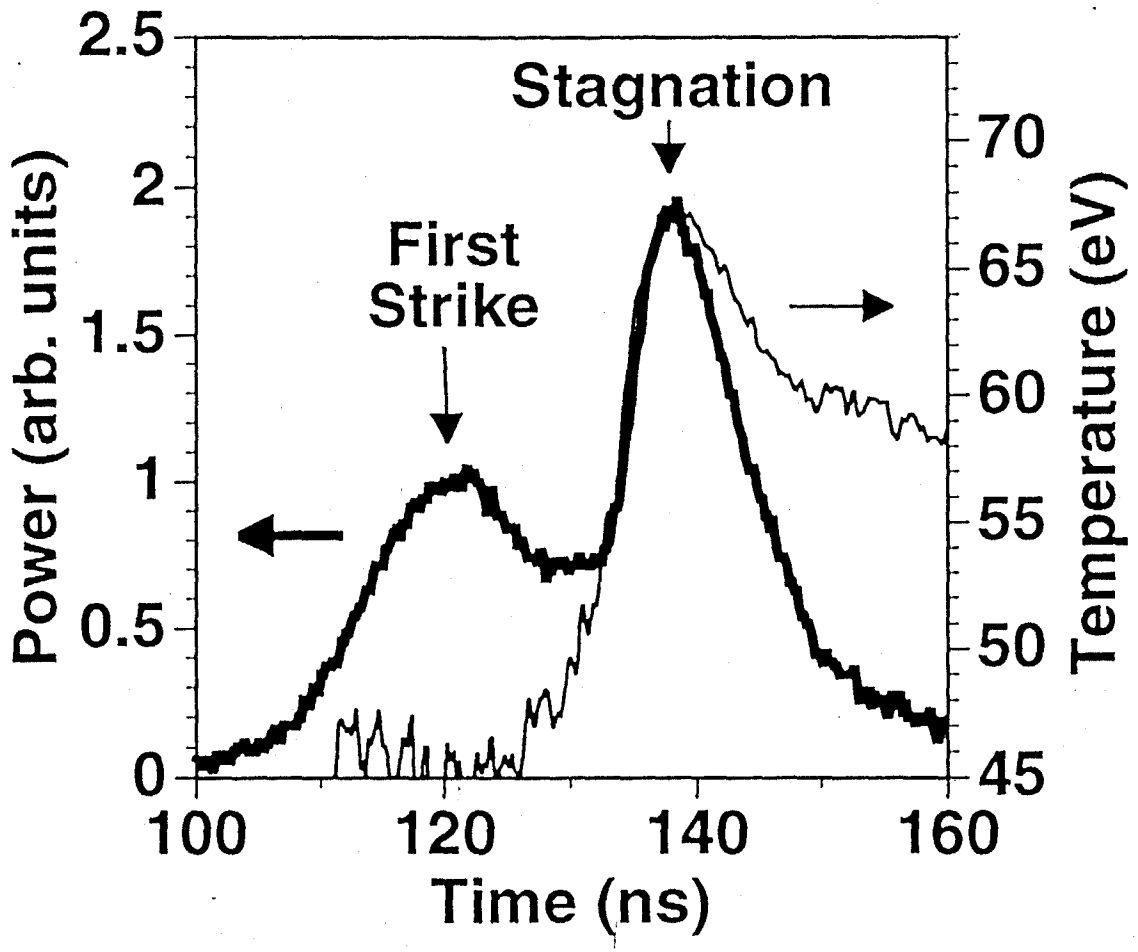
Stagnation
First
Strike
Power (arb. units)
Temperature (eV)
Time (ns)
2.5
2
1.5
1
0.5
0
70
65
60
55
50
45
100
120
140
160

Fig 2

# Z Hohlraums with Foam-Filled Pulse-Shaping Targets Demonstrate Flexibility in Producing a Range of Required NIF Foot-Pulses

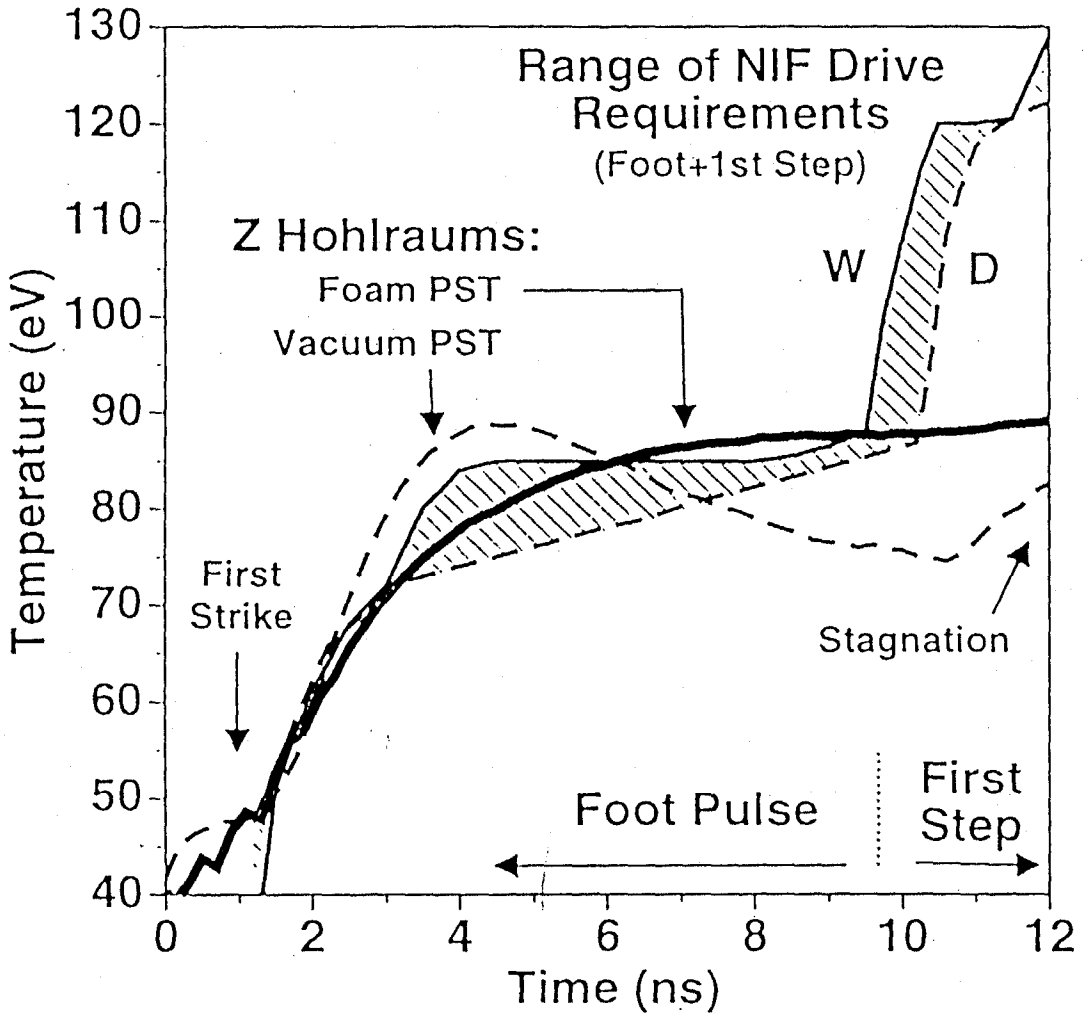


TWLS+REO 6/9/99

Fig. 3

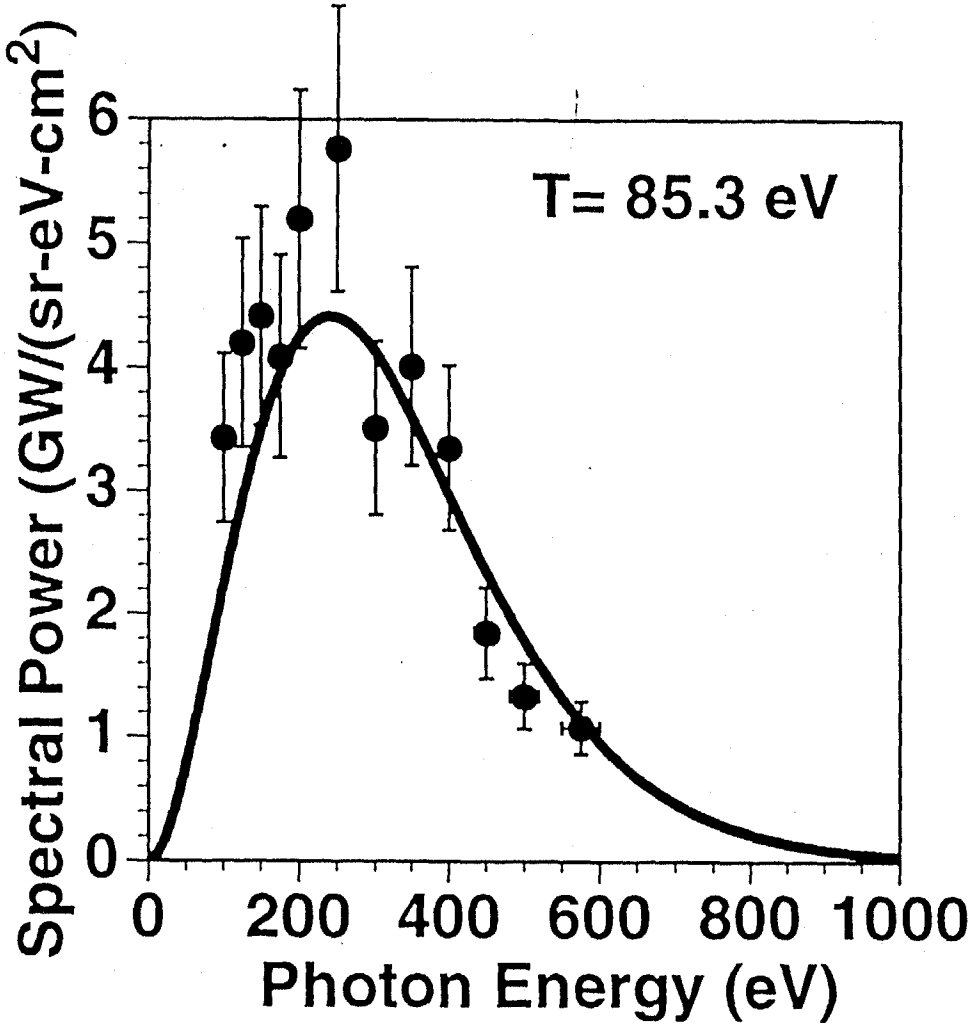
T= 85.3 eV
Spectral Power (GW//(sr-eV-cm2)
0
1
2
3
4
5
6
0
200
400
600
800
1000
Photon Energy (eV)

Fig 4

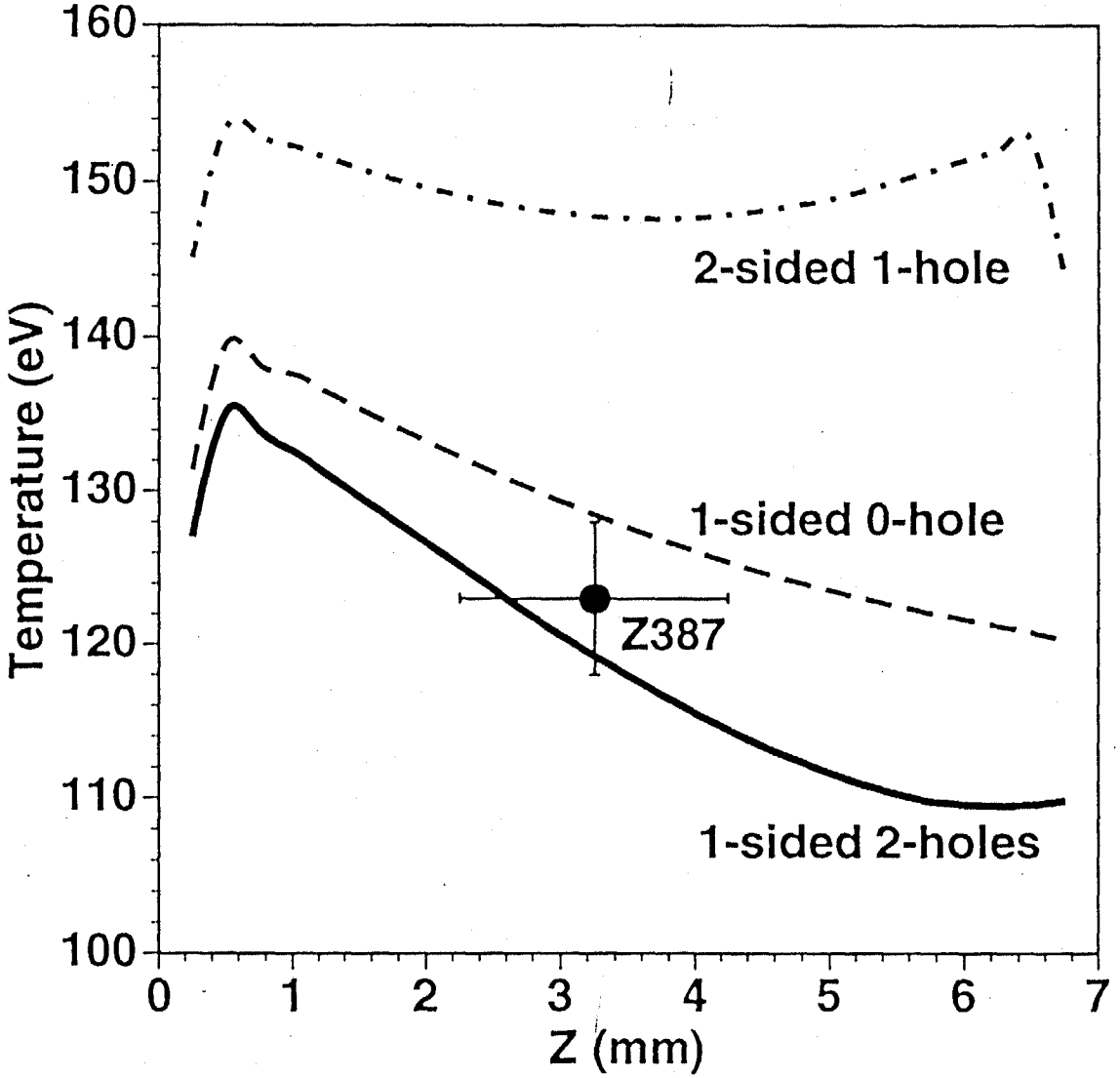
160
150
140
130
120
110
100
Temperature (eV)
2-sided 1-hole
1-sided 0-hole
Z387
1-sided 2-holes
0
1
2
3
4
5
6
7
Z (mm)

Fig 5

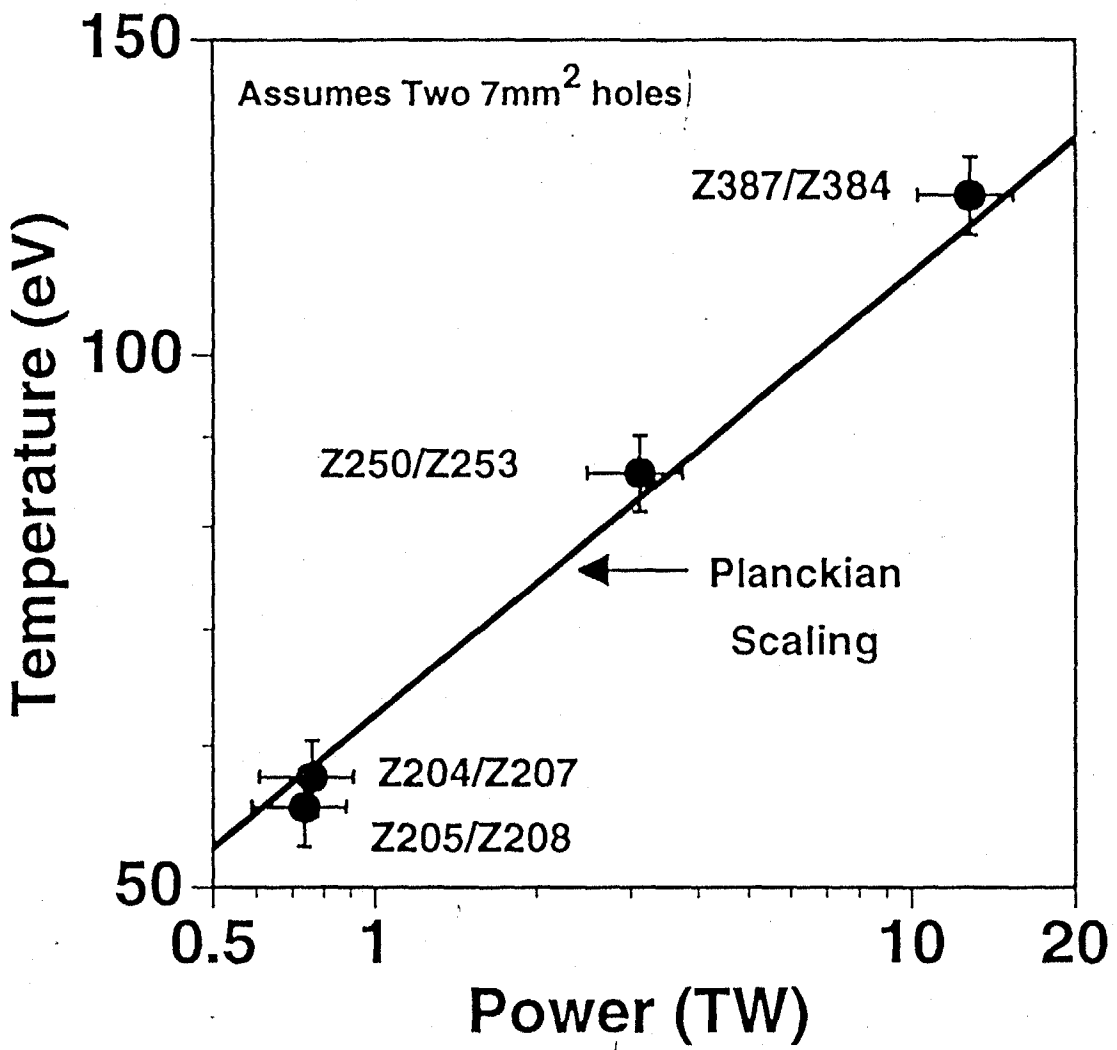
150
100
50
Temperature (eV)
Assumes Two 7mm$^2$ holes
Z387/Z384
Z250/Z253
Planckian
Scaling
Z204/Z207
Z205/Z208
0.5
1
10
20
Power (TW)

Fig 6